Multifunctional, smart, non-Newtonian polymer matrix with improved anti-impact properties enabling structural health monitoring in composite laminates

Konstantinos Myronidis[1], Marco Boccaccio[1], Michele Meo[1], Fulvio Pinto[1]
Department of Mechanical Engineering, University of Bath, Bath BA2 7AY, UK
km515@bath.ac.uk

Abstract. Autonomous Structural Health Monitoring (SHM) has been introduced in composite structures extensively over the last decade in an attempt to proactively monitor potential internal defects, however active/passive control of their integrity status still remains a challenge. In this work, a novel, non-Newtonian multifunctional polymer with unique active/passive capabilities is proposed for impact protection and SHM of composite laminate structures. This Polyborosiloxane(PBS)-based polymer with unique shear-dependant energy absorption characteristics, owed to a phase transition occurrence within its polymeric network, was utilised as scaffold for ferromagnetic iron particles which enabled the manufacturing of the multifunctional matrix for Glass Fibres Reinforced Polymer (GFRP). The iron particles were positioned in the polymer matrix, which was reinforced with glass fibres and employed as outer ply of a laminate structure. Their presence enables a dual functionality of the multifunctional layer: firstly, in the presence of a magnetic field, triggers the phase transition of the polymeric network offering protection to the laminate in case of impacts, and secondly, post-impact allows for the assessment of the internal integrity of the component, acting as an embedded heat source for active Infrared (IR) Thermography. The ability of the iron particles to initiate the phase transition was investigated by means of Low Velocity Impact in the presence/absence of a magnetic field and the laminates were then examined by means of induction thermography, for the evaluation of the internal damage. Results revealed that iron particles in the presence of a magnetic field led to an enhanced protection of the composite laminates, significantly reducing the extent of the internal damage. This novel, low-cost multifunctional layer provides a unique solution for the protection of composite materials, addressing their inherent weak resistance in out-of-plane direction and providing affordable SHM, thus opening new perspectives for smart structural materials which are in great demand in engineering sectors.

Keywords: SHM, GFRP, SSG, LVI, Induction Thermography.

1 Introduction

1.1 Structural Health Monitoring (SHM)

Composite materials have become the first-choice material in engineering sectors such as transportation and wind energy, predominantly due to their exemplary specific mechanical properties and fatigue performance, with the growth of the global market for these materials estimated to further increase in the forthcoming years [1]. The excellent specific mechanical properties of composites structures are primarily owed to the reinforcements employed in these, most commonly in the form of Carbon or Glass fibres. However, the effectiveness of their load-bearing capabilities is mainly in the in-plane direction of the fibres, with the lack of reinforcements in the out-of-plane direction resulting into poor response in such loading conditions. In the event of out-of-plane loading conditions, such as Low Velocity Impacts, damage inflicted onto a laminate may remain concealed, resulting in undetectable Barely Visible Impact Damage (BVID), that can have detrimental effects on the entire structure and may lead to its catastrophic failure. Thus, in order to improve the safety of composite structures, assess damage extent and reduce maintenance expenses, structural health monitoring and non-Destructive evaluation can be deemed essential [2, 3].

Various SHM and NDE techniques have been employed in polymer composite structures for the prediction and evaluation of damage. Some of the most prominent SHM techniques include the implementation of Eddy-current [4, 5], piezoelectric [6, 7] and acoustic sensors [8], whereas various forms of thermography such as infrared (IR) [9], have been proven to be cost-efficient and accurately evaluate the extent and localisation of potential defects. IR thermography can be classified either as passive, where the materials inspected are not in thermal equilibrium, and active, where an external excitation source, such as an electromagnetic source, is employed to generate heat into the component. The use of IR cameras enables the monitoring of temperature gradients on the surface of composite structures and provides information on their structural health. However, one of the major disadvantages of IR thermography for composites is the need for external heat sources, which forces parts to be dismantled in order to be inspected and constitute a costly operation especially in case of large structures such as for aerospace or railways applications that are not easily accessible to the inspectors. Several studies have been proposed over the years to overcome this issue by exploiting the presence of additional phases embedded within the laminate thickness to provide an internal heat source and enable in situ thermography [9], in some cases, also providing an improvement of impact resistance such as in the case of embedded Shape Memory Alloys wires [10]. Despite the excellent results of these studies however, the possibility to enable these features without using expensive metal-based grids but rather using an active multifunctional polymer, constitutes an attractive alternative as it would reduce the additional weight given by the embedded heat source while also lowering manufacturing complexity and, consequently, production and maintenance costs.

1.2 Shear Stiffening Gel (SSG)

Shear Stiffening Gels are non-linear polymeric materials, with their properties being rate-dependant, and possess admirable energy absorption capabilities. The formulation of SSGs is based on the reaction of a polydimethylsiloxane (PDMS) precursor with boric acid, which results in a dynamic covalent polyborosiloxane network, which is crosslinked reversibly by boron-oxygen bonds [11, 12]. SSGs in near equilibrium state and with no stresses applied on these, will slowly deform, as the polymeric network of siloxane chains and boron-oxygen (B-O) covalent bonds will gradually expand. The application of a strain at slow rates on SSGs will initiate a transition to a viscous state; the siloxane chains at these strain rates will have sufficient time to stretch and a small number of boron -oxygen bonds will break [13]. An increase on the applied strain rate will impose a phase transition of the material, from viscous to rubbery state. At this stage, a dynamic breaking and reformation of the covalent B-O bonds is taking place, enabling the SSG to absorb energy due to friction in the polymeric chain network, which macroscopically translates to a rise of the SSGs stiffness [14-16]. Finally, a strain introduced at higher rates will allow for another phase transition from rubbery to glassy state, however at these rates yielding and rupture occurs at the siloxane chains[17].

The prominent energy absorption characteristics of SSGs have been employed primarily in anti-impact applications in composite structures, in an attempt to improve their impact resistance [18]. Wang et al. [19] prepared a Kevlar fabric impregnated with SSG, by a simple “Dip’n’Dry” method, where the SSG was dissolved in a solvent and the fabric was immersed in the solution, in order to fill the gaps of the weave, which drastically improved the stab and yarn-pull performance of the fabric when this was compared to neat Kevlar. In addition to this method, the also proceeded to the addition of carbon nanotubes, effectively creating an electrically conductive material. The addition of conductive particles in SSGs evidently improved their performance, as it was shown that their properties are not only rate-dependant, but with the addition of carbonyl iron (CI) particles and/or carbon nanotubes, can also become dependent on the intensity of an applied magnetic field [20, 21]. Both these studies investigated the response of SSGs containing conductive materials, in the presence/absence of magnetic fields and under a wide range of induced rates, and from the results it is clear that the presence of a magnetic field results in the improvement of the properties of the material. The proposed mechanism suggested in these works is that the presence and intensity of the magnetic field drives the conductive particles to form magnetic chains, promoting the reaction between the siloxane chains and obstructing their disentanglement, as described in the mechanism of SSGs.

Based on these premises, it is evident that the incorporation of conductive particles in SSGs can lead to the creation of a multifunctional smart layer. The outstanding energy absorption capacity of SSGs can be further improved with the addition of conductive materials, which in turn can be also exploited for structural health monitoring purposes, in order to not only improve the protection against impact loads, but also provide a quick and easy preliminary assessment of the internal health state of the component after an impact event.

Based on these considerations, in this work, a smart SSG-based multifunctional matrix containing iron particles was used in conjunction with a dry glass fibres layer and placed on the surface of a GFRP laminate during the layup procedure; this proposed multifunctional layer can provide an active/passive improved impact resistance on the laminate in the presence/absence of a magnetic field, while at the same time the presence of the conductive particles is able to enable SHM features into non-conductive composite materials such as GFRPs, via means of induction thermography without the need for bulky and expensive external heat sources.

2 Materials and Methods

2.1 Materials

The manufacturing of the laminates employing the multifunctional matrix involved various stages; at a first stage the SSG was synthesised, followed by a "Dip'n'Dry" method on a single glass fibre layer, at which stage the iron particles were also introduced. Finally, glass fibre laminates were prepared with a wet lay-up method and the multifunctional layer was positioned as the outer layer during the layup procedure.

In particular, PDMS with initial kinematic viscosity of 50 cSt and boric acid with stoichiometric ratio of boron to silicon of 0.8 were combined in the presence of ethanol, which promoted the homogenisation of the solution. The mixture was heated in a conventional oven for 72 hours at 180 C°, upon which it was cooled down in room temperature. The resulting SSG demonstrated significantly different properties to its precursor, with increased viscosity and opaque colour.

At a second stage, the SSG was dissolved in ethanol, and a single layer of glass fabric was inserted into the solution; a spiral-shaped mask was used at this stage for the dispersion of the iron particles, which allowed for a defined pattern that can improve the properties of the SSG on demand via the application of a magnetic field and that can be easily used for induction heating during SHM analyses.

The glass fibre laminates employed in this work were a 2x2 twill weave, with four layers prepared via wet layup method and epoxy resin. The multifunctional layer was positioned on the top surface of the laminates while the consolidation took place in an autoclave. It is important to underline that the presence of the multifunctional layer did not affect the curing reaction of the laminates that were cured together with the control samples.

Two different configurations of samples were manufactured, a control configuration with five layers of glass fibres, hereinafter named GL, and one configuration employing the multifunctional matrix as a top layer. In order to investigate the effect of the magnetic field on the impact performance of the smart matrix, the samples of the latter configuration were duplicated, with samples impacted without a magnetic field denoted as SN-xx and samples impacted at the presence of a magnetic fields denoted as SF-xx.

2.2 Methods

Rheology

The ability of the SSG to store energy was investigated with oscillatory rheological measurements. A DHR-2 rheometer from TA instruments with a 25 mm parallel plate configuration was employed to conduct measurements over a frequency range between 0.1 and 100 Hz. A small constant compressive load of 0.1 N on the samples during the procedure was used in place of monitoring the gap between the plates, due to initial viscous state of the SSG. The resultant storage (G') and loss (G'') moduli were drawn in logarithmic scales over the examined frequencies.

Low Velocity Impact (LVI)

The dimension of the samples were 150x100 mm according to the ASTM 7136 international standard [22], with three samples tested per configuration. A drop-weight tower employing a shuttle moving on low friction rails, with a hemispherical tip of 15mm and weight of 2.66 kg was used. The data from the impact events were recorded with a load cell, positioned behind the hemispherical tip, and via an oscilloscope stored in a PC. With the use of (Eq.1) where E is impact energy in J, m is the mass of the shuttle in kg, g the gravitational acceleration in ms^{-2} and h the shuttle's release height, the impact energy of 5 J was achieved by adjusting the height of the shuttle.

$$E = mgh \qquad \textbf{Eq.1}$$

All data obtained were postprocessed via MatLab in order to obtain force-displacement curves of the samples and evaluate the amount of absorbed energy, by double integration of the force-time data. The multifunctional samples were tested in the presence/absence of a magnetic field. A schematic illustration of the experimental setup can be viewed in Figure 1.

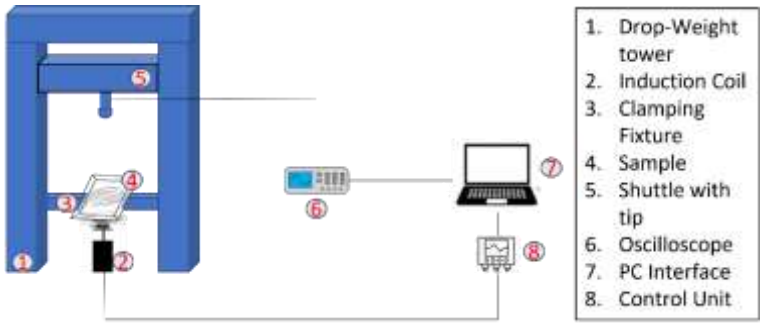

Figure 1 Schematic representation of low velocity impact setup employing a magnetic field.

Induction Thermography

Active Infra-Red (IR) thermography has been widely employed for detection of surface and internal flaws[23, 24]. In these methods, the external surface of a component is subjected to an ultrasonic excitation or a heat source and then an IR camera is used to reveal any irregular heat distribution along the surface of the samples being inspected. Among the other thermography-based techniques, induction heating is a well-suitable method for heat generation in electrically conductive materials [25, 26]. Heat generation occurs when an alternate current is applied to a coil of a conductive material, thus producing a time variable magnetic field. When the conductive material is placed in the close proximity of this primary magnetic field, eddy currents are generated which generates a secondary magnetic field, and heat. The eddy currents tend to propagate along the surface of the inspected component (skin effects), which can be quantified with the penetration depth δ, that is the depth location were eddy current field is decreased by 37%. This can be estimated as follows[27]:

$$\delta = \sqrt{\frac{1}{\pi \mu \sigma f}} \qquad \textbf{Eq.2}$$

Where μ is the magnetic permeability, σ represents the electrical conductivity and f is the current's frequency. The heated component behaves as an ohmic resistor, with the induced heat being proportional to the generated power P, which can be defined by:

$$P = \frac{(2\pi f \mu H A)^2}{R} \qquad \textbf{Eq.2}$$

Where H represents the magnetic field intensity, A is the sectional area and R is the electrical resistance of the material. For the inspection, an induction system is used in conjunction to an IR camera to perform active NDT thermography inspections on the inspected sample. The heat is provided by the induced electric field due to the presence of the iron particles embedded in the multifunctional layer on the surface of the laminate. An illustration of the experimental setup employed for IR induction thermography is depicted in Figure 2.

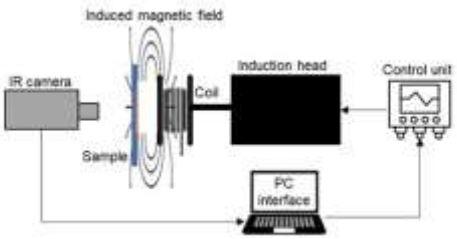

Figure 2 Schematic representation of IR induction thermography experimental setup.

During LVI and IR induction thermography the iron particles were heated up with a current of 6.4 A and a frequency of 290 kHz.

3 Results and Discussion

3.1 Results

Rheology

The resulting storage (continuous blue line) and loss (dashed blue line) moduli can be seen in Figure 3, with the red marker indicating the intersection point between the moduli.

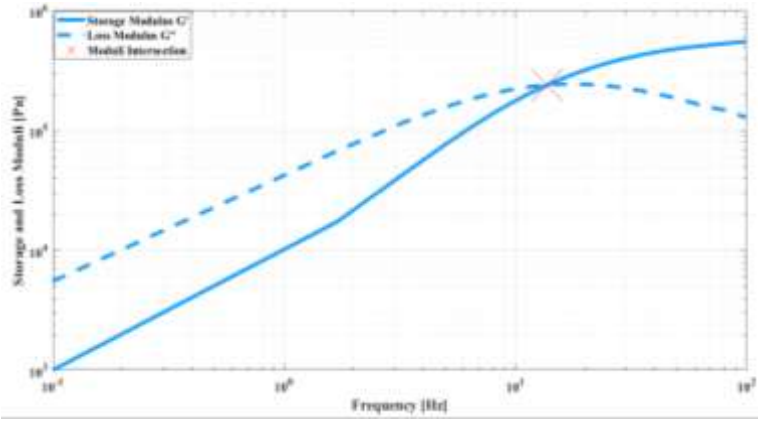

Figure 3 Oscillatory rheological measurements of SSG with storage modulus in continuous blue line, loss modulus in dashed blue line and point of intersection marked with red marker.

The analysis of the curves of the SSG reveals a material whose properties are frequency dependant; at the beginning of the measurements, G' recorded values considerably lower than those of G'', in the 1 kPa region. These values indicate a soft material, which due to its viscoelastic nature dissipates energy in the form of heat losses. As the induced rates on the SSG are increased, so do the values for both moduli, until approximately 13.7 Hz where they intersect, and storage modulus becomes predominant whereas loss modulus values start decreasing. Up until this point the material remained at a viscous state, however, at the intersection of the moduli a phase transition occurs and the elastic properties of the material prevail. At a microscopic level, the dynamic breaking and reformation of the boron-oxygen bonds now takes place, obstructing the disentanglement of the siloxane chains, whereas macroscopically this translates to a rise in stiffness and a solid-like behaviour. The final value of storage modulus recorded for the SSG was approximately 550 kPa, an increase of 550% clearly indicating the material's ability to change its mechanical properties in response to an external stimulus, thus resulting in an additional energy absorption mechanism.

Low Velocity Impact

In Figure 4 all samples impacted at an energy level of 10 J are depicted, with circles indicating the maximum forces recorded and arrows their trends.

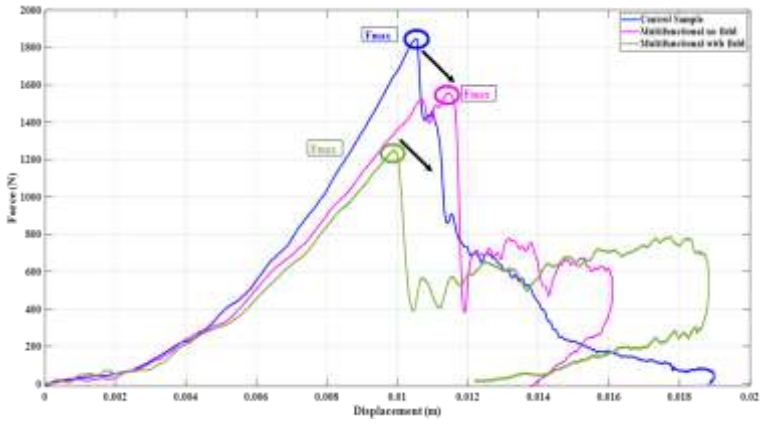

Figure 4 Force-displacement curve obtained from an impact energy level of 10 J. Sample GL in blue line, SN in purple line and SF in green line

The evolution of the curve for the control sample (blue line) suggests that the sample has sustained complete perforation, indicated by an open curve. The maximum force attained by the sample (Fmax) was recorded at 1845 N, with the maximum displacement at 0.019 m. The amount of absorbed energy was evaluated at 9.98 J, denoting the inability of the target to offer any resistance to the impact event. The multifunctional sample impacted in the absence of a magnetic field revealed partial penetration and a closed curve, with Fmax in this case recorded at 1554 N, approximately 16% lower than the previous sample. The maximum displacement achieved by this sample was 0.016 m and the amount of absorbed energy was estimated at 9.6 J. The multifunctional sample impacted in the presence of a magnetic field recorded significantly reduced Fmax compared to the previous samples, 20% and 33% respectively, an observation also seen in similar research activities in which the impacted side of the sample contained SSG [16]. The maximum displacement reached similar values of the control sample however in this case, this was not accompanied by the perforation of the sample that instead kept its integrity. The amount of absorbed energy was estimated at 9 J, approximately 10% and 6% reduced, in comparison to the control and other multifunctional sample. All values of interest have been tabulated in Table 1 below.

Table 1 Values of interest obtained during LVI tests on samples.

Sample	Fmax [N]	Max displacement [m]	Absorbed energy [J]
Control	1845	0.019	9.98

Multifunctional no field (SN)	1554	0.016	9.60
Multifunctional with field (SF)	1249	0.018	9.05

Post-impact, a visual inspection of the samples was conducted with images obtained from either side of the samples which are depicted in Figure 5.

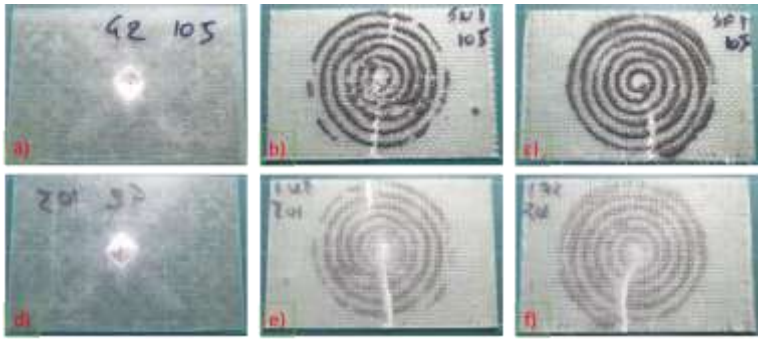

Figure 5 Samples post-impact. Impacted side on top row a) control sample, b) multifunctional sample with no magnetic field applied and c) multifunctional sample with magnetic field applied. Bottom row with opposite side of impact d) control sample, e) multifunctional sample with no magnetic field applied and f) multifunctional sample with magnetic field applied.

The visual inspection of the samples further corroborated the results of LVI; the control sample (Figure 5a and Figure 5d), appeared to have sustained complete perforation, revealing an inability to resist deformation, suggested by the prolonged damaged area at the location and around impact. In the absence of a magnetic field, the multifunctional sample (Figure 5b and Figure 5e), appeared to have resisted perforation, however with straightforward evidence of prolonged damage and partial penetration. The magnetic field during impact appears to have beneficial effects on the response of the second multifunctional sample as illustrated in Figure 5c and Figure 5f. Indeed, by comparing the results from the SN and SF samples, the damage inflicted on the sample subjected to the latter appears significantly reduced compared to the previous one which can only be attributed to the effect of the magnetic field on the properties of the SSG, due to the presence of iron particles.

Thermography

The tests were performed on the two impacted multifunctional samples. Figure 6a shows the IR image captured for the impacted multifunctional sample with no magnetic field applied during the impact event (SN). The damage regions are clearly highlighted in the centre of the spirals, as well as the delamination propagated towards the left and right edge. Results from the thermography inspection conducted on the impacted multifunctional samples (SF) as the magnetic field was applied during the impact (see

Figure 6b), showed a smaller heat distribution inhomogeneity compared to the previous case, which is the result of the activation of the stiffening properties given by the excited iron particles.

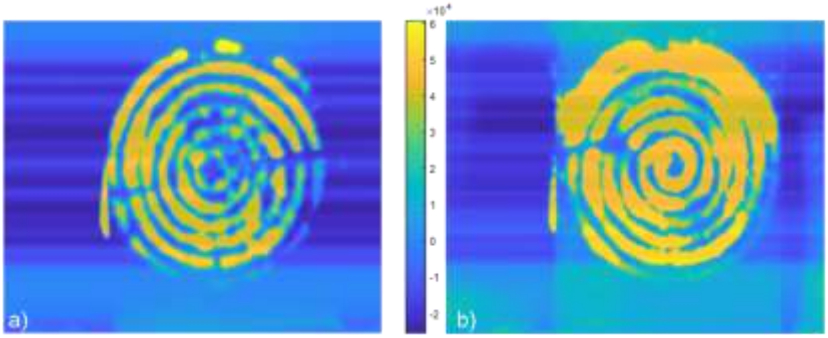

Figure 6 IR induction thermography imaging, a) multifunctional sample with no magnetic field applied (SN) and b) multifunctional sample with magnetic field applied (SF).

3.2 Discussion

A deeper analysis of all results of this experimental campaign can reveal some further insights. The rheological measurements of the SSG showed clear rate-dependant properties and an ability to store energy at increasing rates of deformation. The employment of the SSG-based multifunctional layer on the outer surface of the samples, clearly improved their impact resistance, resulting in optimised energy absorption characteristics. Indeed, while the control samples absorbed greater amounts of energy this was consumed primarily as damage energy due to the opening of new surfaces in the form of fibre/matrix failure and delamination. Both multifunctional samples recorded significantly lower Fmax values (16% and 33% respectively) compared the control sample and similar values of maximum displacement showing a more ductile response. These values, in conjunction with the absence of signs of complete perforation in the modified laminates, indicate that the presence of the of the multifunctional layer completely altered the behaviour of the laminates, changing the way the impact energy is distributed within the samples due to the phase transition within the SSG.

The presence of iron particles and their ability to further improve the mechanism of the SSG in the presence of a magnetic field was evident in the results of LVI and the visual inspection of the samples. The Fmax recorded for the SF sample was reduced approximately by 20% compared to the SN sample, with a 6% reduction in the amounts of absorbed energy as well. These results were further corroborated from the IR induction thermography, where lower heat distribution inhomogeneities were revealed in close proximity of the impact area of the SF samples in comparison with the SN ones which is a clear sign of the reduction of the extent of the internal delamination caused by the enhancement of the phase transition mechanism given by the presence of the applied magnetic field.

4 Conclusions

In this work, a novel, multifunctional layer for composite structures characterised by excellent energy absorption properties and SHM features is proposed. This smart material is based on a glass fibres layer impregnated with an SSG polymer in which conductive particles are arranged in a spiral pattern to enhance the phase-transition within the SSG, thus improving its energy absorption characteristics. At the same time the presence of the conductive material allows for a rapid assessment of the internal integrity of the laminate via acting as an embedded heat source during induction thermography, reducing the costs associated with thermal inspection of large composite components that usually require expensive external heating systems.

The polyborosiloxane-based SSG material was synthesised with PDMS and boric acid, and its ability to store energy was validated with rheological measurements. Employing a "Dip'n'Dry" method glass fibre fabrics were prepared with the SSG acting as a matrix and iron particles were positioned at this stage in a spiral configuration using a 3d printed mask. The laminates were then mapped via means of induction thermography and then subjected to LVI, at an energy level of 10 J. The interpretation of the results from LVI conjointly with the visual appearance of the samples post-impact, indicated that the exemplary protection offered to the laminates by the SSG can be further improved in the presence of a magnetic field. These results were confirmed with the use of IR induction thermography, where a reduction of the internal damage extent is evident.

The results from this experimental campaign demonstrates that the proposed SSG-based multifunctional layer provides a unique solution for composite structures, addressing the inherent problematic of their weak resistance against out-of-plane loadings while at the same time providing affordable SHM inspection. By tackling these two drawbacks of traditional composite structures, this multifunctional layer opens new perspectives for multifunctional, smart structural materials which are in great demand in an increasing number of engineering sectors.

5 Funding

The work in this publication was conducted under the project with title "Aegis, Advanced Energy-Absorption Polymer for Impact-Resistant Smart Composites" funded by the Engineering and Physical Sciences Research Council (EPSRC) [EP/T000074/1].

6 References

[1] V.M. Reasearch, 2021 Statistics: U.S. and Global Composite Materials Market Will Surpass $ 128.82 Billion at 7.52% CAGR Growth: Vantage Market Research (VMR), (2021).
[2] D. Balageas, C. Fritzen, A. Guemes, Structural health monitoring (London: ISTE), (2006).
[3] C. Boller, F.-K. Chang, Y. Fujino, Encyclopedia of structural health monitoring, Wiley Online Library2009.
[4] D. Placko, I. Dufour, A focused-field eddy current sensor for nondestructive testing, IEEE transactions on magnetics 29(6) (1993) 3192-3194.
[5] D.J. Sadler, C.H. Ahn, On-chip eddy current sensor for proximity sensing and crack detection, Sensors and Actuators A: Physical 91(3) (2001) 340-345.
[6] S.S. Kessler, S.M. Spearing, C. Soutis, Damage detection in composite materials using Lamb wave methods, Smart materials and structures 11(2) (2002) 269.
[7] X.P. Qing, S.J. Beard, A. Kumar, T.K. Ooi, F.-K. Chang, Built-in sensor network for structural health monitoring of composite structure, Journal of Intelligent Material Systems and Structures 18(1) (2007) 39-49.
[8] J.P. McCrory, S.K. Al-Jumaili, D. Crivelli, M.R. Pearson, M.J. Eaton, C.A. Featherston, M. Guagliano, K.M. Holford, R. Pullin, Damage classification in carbon fibre composites using acoustic emission: A comparison of three techniques, Composites Part B: Engineering 68 (2015) 424-430.
[9] F. Ciampa, P. Mahmoodi, F. Pinto, M. Meo, Recent advances in active infrared thermography for non-destructive testing of aerospace components, Sensors 18(2) (2018) 609.
[10] F. Pinto, F. Ciampa, M. Meo, U. Polimeno, Multifunctional SMArt composite material for in situ NDT/SHM and de-icing, Smart Materials and Structures 21(10) (2012) 105010.
[11] F.V. Drozdov, S.A. Milenin, V.V. Gorodov, N.V. Demchenko, M.I. Buzin, A.M. Muzafarov, Crosslinked polymers based on polyborosiloxanes: Synthesis and properties, Journal of Organometallic Chemistry 891 (2019) 72-77.
[12] N. Seetapan, A. Fuongfuchat, D. Sirikittikul, N. Limparyoon, Unimodal and bimodal networks of physically crosslinked polyborodimethylsiloxane: viscoelastic and equibiaxial extension behaviors, Journal of Polymer Research 20(7) (2013) 1-9.
[13] M.J. Ballard, R. Buscall, F.A. Waite, The theory of shear-thickening polymer solutions, Polymer 29(7) (1988) 1287-1293.
[14] Z. Liu, S.J. Picken, N.A. Besseling, Polyborosiloxanes (PBSs), synthetic kinetics, and characterization, Macromolecules 47(14) (2014) 4531-4537.
[15] M. Tang, W. Wang, D. Xu, Z. Wang, Synthesis of Structure-Controlled Polyborosiloxanes and Investigation on Their Viscoelastic Response to Molecular Mass of Polydimethylsiloxane Triggered by Both Chemical and Physical Interactions, Industrial & Engineering Chemistry Research 55(49) (2016) 12582-12589.
[16] S. Zhang, S. Wang, T. Hu, S. Xuan, H. Jiang, X. Gong, Study the safeguarding performance of shear thickening gel by the mechanoluminescence method, Composites Part B: Engineering 180 (2020) 107564.
[17] W. Jiang, X. Gong, S. Wang, Q. Chen, H. Zhou, W. Jiang, S. Xuan, Strain rate-induced phase transitions in an impact-hardening polymer composite, Applied Physics Letters 104(12) (2014) 121915.

[18] C. Zhao, X. Gong, S. Wang, W. Jiang, S. Xuan, Shear Stiffening Gels for Intelligent Anti-impact Applications, Cell Reports Physical Science 1(12) (2020) 100266.
[19] S. Wang, S. Xuan, M. Liu, L. Bai, S. Zhang, M. Sang, W. Jiang, X. Gong, Smart wearable Kevlar-based safeguarding electronic textile with excellent sensing performance, Soft Matter 13(13) (2017) 2483-2491.
[20] Y. Wang, S. Wang, C. Xu, S. Xuan, W. Jiang, X. Gong, Dynamic behavior of magnetically responsive shear-stiffening gel under high strain rate, Composites Science and Technology 127 (2016) 169-176.
[21] X. Fan, S. Wang, S. Zhang, Y. Wang, X. Gong, Magnetically sensitive nanocomposites based on the conductive shear-stiffening gel, Journal of Materials Science 54(9) (2019) 6971-6981.
[22] D. ASTM, 7136/D 7136M, Standard test method for measuring the damage resistance of a fibre-reinforced polymer matrix composite to a drop-weight impact event (2007).
[23] T. Sakagami, S. Kubo, Applications of pulse heating thermography and lock-in thermography to quantitative nondestructive evaluations, Infrared Physics & Technology 43(3-5) (2002) 211-218.
[24] T. Inagaki, T. Ishii, T. Iwamoto, On the NDT and E for the diagnosis of defects using infrared thermography, NDT & E International 32(5) (1999) 247-257.
[25] F. Flora, M. Boccaccio, G.P.M. Fierro, M. Meo, Non-destructive thermography-based system for damage localisation and characterisation during induction welding of thermoplastic composites, Thermosense: Thermal Infrared Applications XLII, International Society for Optics and Photonics, 2020, p. 114090I.
[26] U. Netzelmann, G. Walle, Induction thermography as a tool for reliable detection of surface defects in forged components, 17th World conference on nondestructive testing, Citeseer, 2008.
[27] R. Rudolf, P. Mitschang, M. Neitzel, Induction heating of continuous carbon-fibre-reinforced thermoplastics, Composites Part A: Applied Science and Manufacturing 31(11) (2000) 1191-1202.